Determining the reduced scattering of skin *in vivo* using sized - fiber reflectometry

T. P. Moffitt and S. A. Prahl

ECE Dept., Oregon Health & Science University, Portland, OR

ABSTRACT

Sized-fiber reflectometry describes a device and method for measuring absorption and reduced scattering of tissue using optical fibers with different diameters. The device used in this paper consists of two fibers with diameters of 200 and 600 micron. Each fiber emits and collects its own backscattered light. Monte Carlo simulations tabulating the diffuse reflectance collected by 200 and 600 micron fibers in a semi-infinite homogenous media are presented for an absorption, μ_a range of 0.2–30 cm^{-1} and a reduced scattering, μ_s' range of 10–200 cm^{-1}. The diffuse reflectance collected by a 600 micron fiber may be approximated by a linear relation to the 200 micron fiber. An empirical relation is derived relating the reduced scattering coefficient to the diffuse reflectance collected with 200 and 600 micron fibers. The sensitivity of the relation is determined for changes in each fiber measurement. Finally, *in vivo* diffuse reflection measurements and reduced scattering coefficient of skin are presented using the aforementioned fiber sizes with a wavelength range of 400–800 nm.

keywords: tissue, reflectance, scattering, absorption, penetration depth.

1. INTRODUCTION

Determining the optical scattering and absorption properties of tissue for diagnostic and therapeutic applications is of interest in medicine. For example, the dosimetry of photodynamic therapy is greatly dependent upon the scattering and absorption properties[1,2] for both light delivery and measurement of drug concentrations. Optical properties have been used to estimate exogenous[3,4] and endogenous[5] chromophore concentrations. Moreover, light scattering and absorption can provide information about both chromophore content and structure, which might be used to distinguish normal and malignant tissues as well as chemical state information[6,7] (e.g. oxy- versus deoxy-hemoglobin). In this regard, an optical biopsy can be performed using optical information of hemoglobin and water content differences in normal and malignant tissue.[8,9]

Several techniques and algorithms have been developed to measure optical properties. Spatially[10–12] and temporally[13–15] resolved measurements have been proposed to extract the optical properties using light distributions based on diffusion theory[16,17] and/or Monte Carlo simulations.[18] A wide variety of algorithms have been explored to extract optical properties including neural network[19] and multiple polynomial regression methods.[20] However, most reflectance techniques rely on light distribution information over a large area ($>1\,\mathrm{cm}^2$) or have separate illumination and collection fibers with a separation distance on the order of several millimeters.

Two studies on devices with separate source and detector fibers show that the mean photon penetration depth increases as the square root of the separation between source and detector fibers either spatially[21] or temporally.[22] Source-detector fiber devices sample relatively large volumes, because of the separation between the fibers.[21,22] Though effort has been made to minimize the sampling volume using small source-detector separations,[23] little work has been done on photon penetration depths when the source fiber is also used to collect backscattered photons.[24] Since large sampling volumes are less likely to be homogenous, to minimize the sampling volume we developed a device that acquires information from small volumes of tissue ($< 1\,\mathrm{mm}^3$) by using the same fiber for both source and detector.

We propose a compact dual-fiber device to make simple and rapid measurements of the absorption and reduced scattering properties of tissue. Each fiber illuminates and collects light independently of the other

Further author information: (Send correspondence to S.A.P.)
S.A.P.: E-mail: prahl@ece.ogi.edu, Telephone: (503) 216-2197, 9205 SW Barnes Rd., Portland, OR 97006, USA

fiber. The device is based on the fact, that in general, tissues with different scattering and absorption properties will scatter different numbers of photons back into a fiber. If only a single fiber is used, two samples with different optical properties could possibly backscatter the same number of photons. This paper proposes a device containing a second, different size fiber to make a second measurement. This second fiber collects information from a different effective volume of the sample than the first fiber.

In this study, we present Monte Carlo simulations of the diffuse reflectance collected by 200 and 600 micron diameter fibers. The tissue is modeled as a semi-infinite and homogenous for an absorption, μ_a range of 0.2–30 cm^{-1} and a reduced scattering, μ_s' range of 10–200 cm^{-1}. We demonstrate that the reflectance collected by a 600 micron fiber may be approximated by a linear relation to the 200 micron where the slope has a functional dependence on the reduced scattering. We show a fit for the slopes as a function of the reduced scattering and show the relative error of the predicted reduced scattering using this slope function in the empirical relation. Diffuse reflectance data is shown for skin on the dorsal side of the forearm. Finally, the reduced scattering of the skin is presented and discussed.

2. MATERIALS AND METHODS

2.1. Sized-Fiber Device

The sized-fiber device uses two bifurcated fibers to separate the illumination light from the back-scattered light (figure 1). The first of these is made by end-coupling two 300 micron diameter fibers onto the face of a 600 micron diameter fiber with SMA connectors. Likewise, the other fiber consists of two 100 micron diameter fibers end-coupled to a 200 micron fiber also using SMA connectors. One each of the 100 and 300 micron fibers were coupled to a tungsten-halogen lamp (LS-1, Ocean Optics, Dunedin, FL) via an SMA connector. The remaining 100 and 300 micron fibers are coupled into a spectrometer (Fluorolog-3, Instruments S.A., Inc., Edison, NJ). The 200 and 600 micron fibers are encased in Teflon tubing with the ends glued together (4011, Loctite Corp., Rocky Hill, CT) and mounted in a SMA connector and polished flush (figure 2). All fibers are fused silica glass/glass from Polymicro Technologies LLC, Phoenix, AZ. The manufacturer cites a numerical aperture of 0.22 which corresponds to a maximum exit angle of 12.7 degrees in air. We measured 13 ± 1 degrees for both the 200 and 600 μm fibers for the maximum acceptance angle in air.

An anodized aluminum baffle is used to block one lamp so that only one fiber illuminates the sample during a spectral scan. The scans were recorded from 400 nm to 800 nm in 1 nm increments; the wavelength range was limited by the emission spectrum of the lamp with a collection slit of 3 nm. The baffle also keeps the lamp output stable since the lamps continuously run throughout the experiments. The baffle is moved to block the other lamp for measurement with the other fiber. The detector end of the fibers are also baffled since both fibers couple into the same detector so that cross-talk is eliminated.

In vivo skin was measured five times with each fiber in the same location on the dorsal side of the arm. Mineral oil was applied to the skin to aid light coupling between the fibers and the skin and fill voids in the stratum corneum. The fiber was held on the arm for one minute before any measurements were recorded to create a consistent pressure induced erythema. The red mark formed by the pressure also simplified repositioning of the fibers in the same location between measurements.

All data points are normalized by using Fresnel reflection from the fiber face in air and water. The voltage returned from the photodiode is converted by

$$\text{Diffuse Reflectance} = \frac{V_{sample} - V_{water}}{V_{air} - V_{water}}[R_{air}(\lambda) - R_{water}(\lambda)] + (R_{water}(\lambda) - 0.04\%)$$

where $\mathrm{R}_{air}(\lambda)$ is the Fresnel reflectance for the fiber core/air junction, $\mathrm{R}_{water}(\lambda)$ is the Fresnel reflectance for the fiber core/water junction at normal incidence and 0.04% is the Fresnel reflectance of tissue with an index of refraction of 1.4 and the fiber core has an index of refraction of 1.457. Measurements of the air and water Fresnel reflectance are taken periodically throughout the experiments to correct for any variations in lamp output.

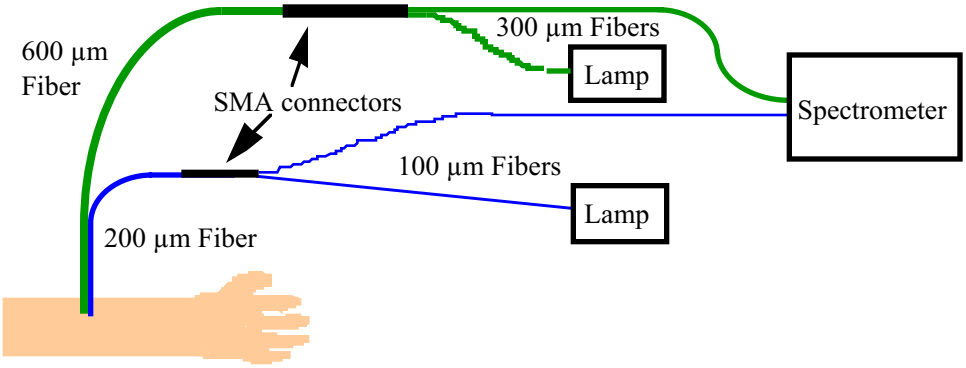

Figure 1. This is a diagram of the sized-fiber device. A pair of bifurcated fibers emit and collect light independently by using baffles on the lamps and the detector.

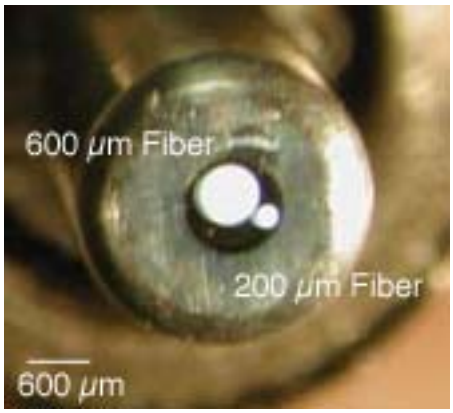

Figure 2. The faces of the 200 and 600 μm fibers are shown mounted together in an SMA connector for use as a handpiece where the fibers were joined using a medical grade epoxy.

2.2. Monte Carlo Simulations

A Monte Carlo program simulated the light collected by a fiber irradiating a semi-infinite homogeneous scattering and absorbing medium. The fiber face was located on the surface of the only boundary included in the simulations. The z-axis coincides with the fiber axis and the face of the fiber is in the $z = 0$ plane. Photons are launched with equal probability over the entire face of the fiber. The direction by which photons are launched is specified by the direction cosines (ν_x, ν_y, ν_z). The angle $\nu_z = \cos\theta_z$ is given a Gaussian distribution that depends on the acceptance angle of the fiber while the other direction cosines are uniformly distributed. The angular distribution approximates the emission from the fibers. Due to under-filled modes, the experimentally measured distribution deviates by 12% from a true Gaussian. The distribution of angles that the photon might take is given by the function

$$p(\theta_z)d\theta_z = \frac{1}{\sqrt{2\pi}} \exp\left(-\frac{\theta_z^2}{2\theta_a^2}\right) d\theta_z$$

where θ_a is the acceptance angle for the fiber. Moreover, the angles were limited such that $\theta_z \leq \theta_a$.

The primary statistic collected by the Monte Carlo program was the fraction of light backscattered into the core of the fiber. Photons which were collected must pass back through the fiber face. Only photons that had an angle less than or equal to the maximum acceptance angle for the fiber were counted into the light collected by the fiber. The maximum acceptance angle for the fiber was input into the program for the fiber in air, then converted using Snell's law for the index of refraction for the incident medium. Photons incident on the fiber face but outside the cone of acceptance were attributed to light lost in the cladding. The acceptance angle was corrected for the index of refraction change of the medium. The index of refraction for the core of the fiber was assumed to be 1.457 as given by the manufacturer's specifications; 1.4 was used for the index of the medium. The index mismatch for both launching and collection was accounted for using the Fresnel reflection for normal incidence introducing an error $\approx 0.02\%$. The anisotropy was chosen to be 0.9 for tissue. In a single simulation, a million photons were launched for each simulation each set of absorption (0.2, 0.5, 1.0, 2.0, 5.0,10.0, 20.0, and 30.0 cm^{-1}) and scattering coefficients (10, 20, 30, 50, 75,100, and 200 cm^{-1}).

3. RESULTS

3.1. Monte Carlo Simulations

The Monte Carlo simulation results of the diffuse reflectance are shown in figure 3 for 200 and 600 micron fibers. In this figure, it is apparent that the 600 micron fiber reflectance is linearly related to the 200 micron fiber reflectance by

$$R_{600} = F(\mu_s')R_{200} - 0.003.$$

where $\mathrm{F}(\mu_s')$ is the slope associated with a particular reduced scattering coefficient. The function, $\mathrm{F}(\mu_s')$, is shown in figure 4 and has the form

$$F(\mu_s') = \frac{25.9}{\sqrt{\mu_s'}} + 0.427.$$

The reduced scattering coefficient is therefore

$$\mu_s'(R_{200}, R_{600}) = \left(\frac{25.9R_{200}}{R_{600} - 0.427R_{200} + 0.003}\right)^2.$$

We test this expression in figure 5 by inputting the Monte Carlo results and comparing the predicted reduced scattering coefficient versus the true reduced scattering coefficient. The relative error for the predicted reduced scattering coefficient is shown in figure 6.

3.2. Skin Measurements

The mean diffuse reflectance mapping for skin *in vivo* is shown in figure 7 over a wavelength range of 400–800 nm. The error bars indicate the standard deviation of five measurements. Figure 8 shows the diffuse reflectance data set converted into the wavelength dependent prediction of the reduced scattering coefficient.

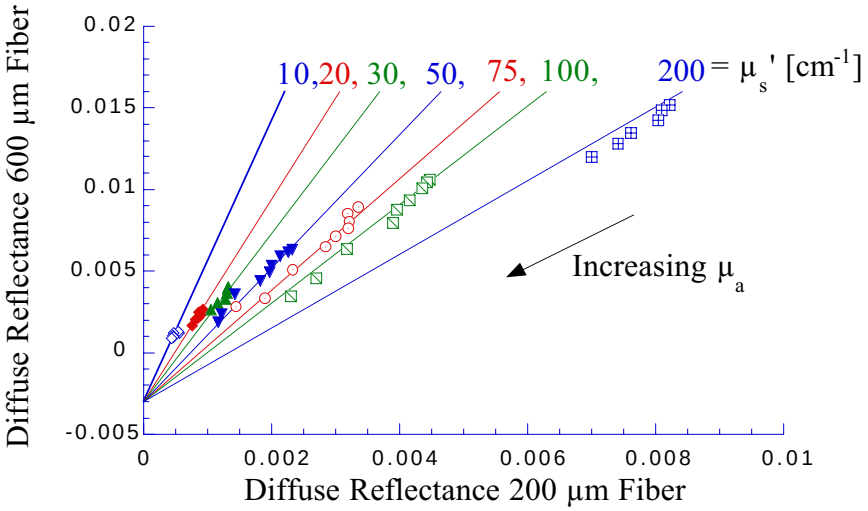

Figure 3. The scattering can be determined from a mapping of the reflectance for each fiber. Each line represents a single reduced scattering coefficient and absorption coefficients increase as the reflectance drops down each line to zero reflectance. For each reduced scattering coefficient, absorption coefficients 0.2, 0.5, 1.0, 2.0, and 5.0 cm^{-1} are shown and for $\mu_s' = 50$, 75, and 100 cm^{-1}, the absorption coefficient range extends to include 10, 20, and 30 cm^{-1} as well.

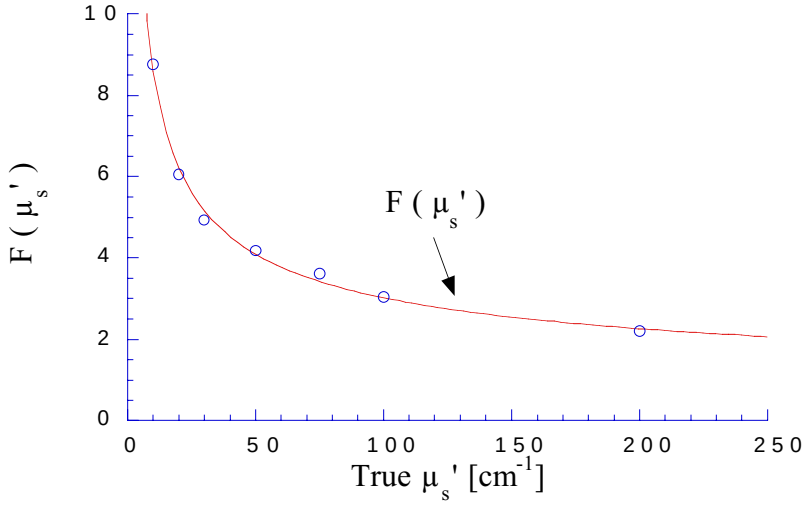

Figure 4: The slope of lines fitted in figure 3 as a function of the reduced scattering coefficient.

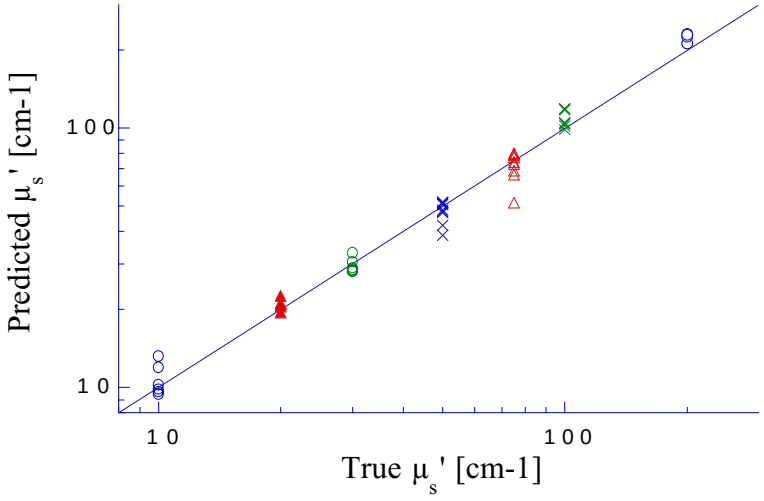

Figure 5. The Monte Carlo simulation diffuse reflectance results are used to compare the predicted reduced scattering coefficients to the true reduced scattering coefficient using the empirical relation relating the reduced scattering coefficient to the diffuse reflectance collected by 200 and 600 micron fibers.

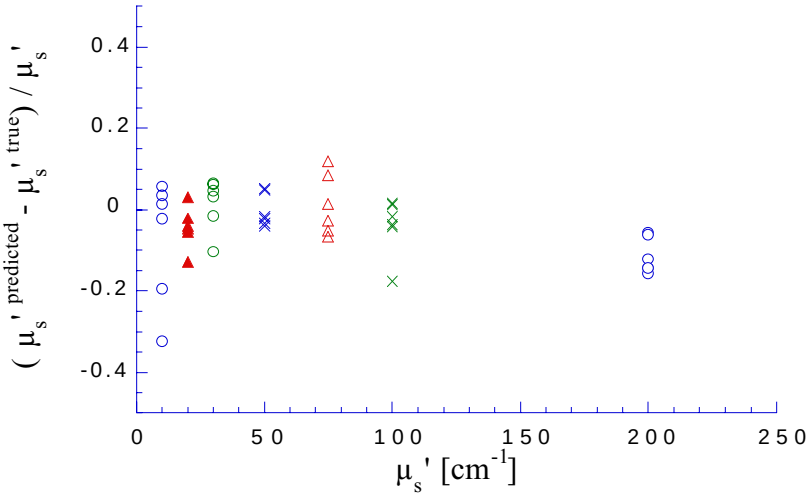

Figure 6. The relative error in the predicted reduced scattering coefficient as a function of the reduced scattering coefficient.

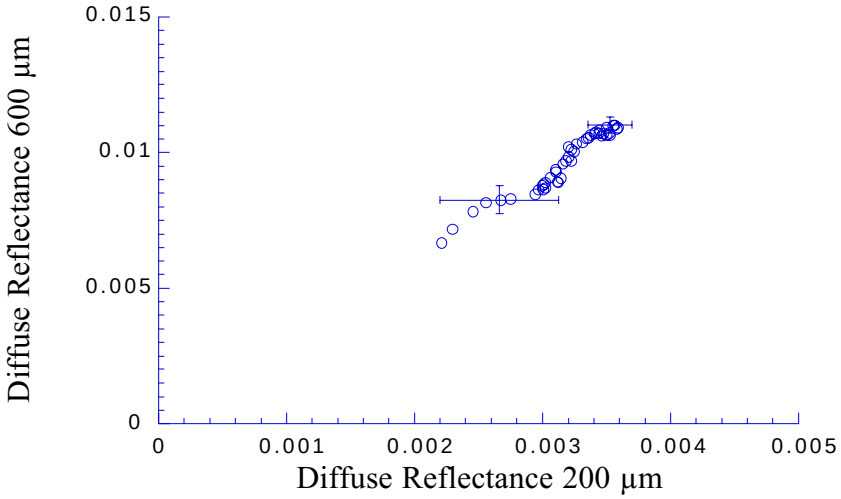

Figure 7: *In vivo* diffuse reflectance for fair skin for the mean of five measurements is shown.

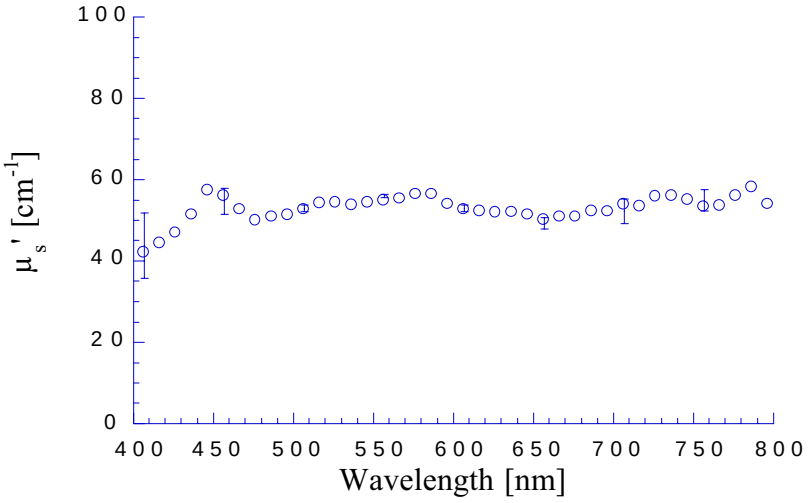

Figure 8. The reduced scattering coefficient is determined for skin *in vivo* using an empirical relation based on Monte Carlo simulations of a semi-infinite homogenous medium.

4. DISCUSSION

The extrapolation of the reduced scattering coefficient could be estimated by a simple empirical relation to diffuse reflectance collected by 200 and 600 micron fibers. Computationally, the reduced scattering was fast to determine and may easily be determined for real-time measurements. The relation worked at reduced scattering coefficients below $10\,\mathrm{cm}^{-1}$ (2 and $5\,\mathrm{cm}^{-1}$ data was no shown) but any error in the diffuse reflectance measurements would translate into very large error in the reduced scattering prediction. The absolute relative error was derived by taking the partial of the empirical relation for the reduced scattering with respect to R_{200} and R_{600}. The relative absolute error is then

$$\frac{\Delta\mu_s'}{\mu_s'} = \frac{2R_{600}}{R_{600}+0.003-0.427R_{200}}\sqrt{\left(1+\frac{0.003}{R_{600}}\right)\left(\frac{\Delta R_{200}}{R_{200}}\right)^2+\left(\frac{\Delta R_{600}}{R_{600}}\right)^2}.$$

The sized-fiber technique is limited in the range of optical properties which may be measured. When the reduced scattering drops below $10\,\mathrm{cm}^{-1}$ then the collected signals are too small to differentiate absorption or scattering. The diffuse reflectance mapping for 200 and 600 micron fibers for fair skin (figure 7) falls within the working reduced scattering range of the device. The wavelength dependence measured using the sized-fiber device does not agree with previous findings for dermis[33] where the scattering decreases with increasing wavelength. We have four possible explanations for our results which are not necessarily exclusive.

First in the model presented here, the tissue is assumed to be homogenous and skin is well known to be a layered tissue. A second possibility is that absorption is influencing the predicted reduced scattering coefficient. The wavelength dependence for the absorption of melanin has nearly the opposite effect on the diffusely reflected light intensity than does the expected wavelength dependence of scattering. The light intensity will be attenuated by melanin absorption in the epidermal layer: attenuated once as light passes through to the dermis and again after returning to the optical fiber from the dermis. In a previous study, the mean depth of photon migration for collected photons was 1.2 and 1.9 reduced mean free paths for the 200 and 600 micron fibers respectively.[34] These depths are roughly 240 and 380 microns respectively using the scattering predicted by the sized-fiber system and assuming that the reduced scattering is greater than absorption. Since the epidermis is about 100 microns thick, this suggests that the majority of the collected photons travel into the dermis.

A third reason may be that the determination of the reduced scattering is frustrated by partial contact of the optical fibers with the tissue. The variation between measurements was grossly different if contact of the fibers to the tissue lacked consistency. Finally, a fourth cause may be that epidermal scattering does not behave the same as dermal scattering with respect to the wavelength. The extraction of the absorption coefficient has yet to be determined but should help to prove or disprove one or more of these explanations for the reduced scattering results.

We have demonstrated that the diffuse reflectance collected by 200 and 600 micron diameter fibers can be used to determine the reduced scattering properties in a semi-infinite medium using an empirical relation. The device is restricted to tissue where the reduced scattering exceeds $10\,\mathrm{cm}^{-1}$. Below this limit, the collected signal is too small to reliably distinguish scattering. The relative error of the predicted reduced scattering properties is less than 20% for absorption ranging 0.2–$30\,\mathrm{cm}^{-1}$.

Acknowledgements

This work was funded by a grant from the National Institutes of Health: NIH-CI-R24-CA84587-01. I would also like to thank Steve Jacques, Jessica Ramella-Roman, and Paulo Bargo for their support and insightful discourse.

REFERENCES

1. B. C. Wilson and M. S. Patterson, "The physics of photodynamic therapy," *Phys. Med. Biol.*, **vol. 26**, pp. 327–360, 1986.

2. B. J. Tromberg, L. O. Svaasand, M. K. Fehr, S. J. Madsen, P. Wyss, B. Sasone and Y. Tadir, "A mathematical model for light dosimetry in photodynamic destruction of human endometrium," *Phys. Med. Biol.*, **vol. 41**, pp. 233–237, 1996.
3. M. S. Patterson, B. C. Wilson, J. W. Feather, D. M. Burns and W. Pushka, "The measurement of dihematoporphyrin ether concentration in tissue by reflectance spectrophotometry," *Photochem. Photobiol.*, **vol. 46**, pp. 337–343, 1987.
4. M. A. O'Leary, D. A. Boas, B. Chance and A. G. Yodh, "Radiation and imaging of diffuse photon density waves using fluorescent inhomogeneities," *J. Lumin.*, **vol. 60–61**, pp. 281–286, 1994.
5. F. F. Jobsis, J. H. Keizer, J. C. LaManna and M. Rosenthal, "Reflectance spectroscopy of cytochrome aa3 *in vivo*," *J. Appl. Physiol.*, **vol. 43**, pp. 858–872, 1977.
6. B. Chance, S. Nioka, J. Kent, K. McCully, M. Fountain, R. Greenfeld and G. Holtom, "Time resolved spectroscopy of hemoglobin and myoglobin in resting and ischemic muscle," *Anal. Biochem.*, **vol. 174**, pp. 698–707, 1988.
7. M. Cope and D. T. Delpy, "System for long-term measurement of cerebral blood and tissue oxygenation on newborn infants by near infrared transillumination," *Med. Biol. Eng. Comput.*, **vol. 26**, pp. 289–294, 1988.
8. J. B. Fishkin, O. Coquoz, E. R. Anderson, M. Brenner and B. J. Tromberg, "Frequency-domain photon migration measurements of normal and malignant tissue optical properties in a human subject," *Appl. Opt.*, **vol. 36**, pp. 10–20, 1997.
9. B. J. Tromberg, O. Coquoz, J. B. Fishkin,, T. Pham, E. R. Anderson, J. Butler, M. Cahn, J. D. Gross, V. Venugopalan and D. Pham, "Noninvasive measurements of breast tissue optical properties using frequency-domain photon migration," *Philos. Trans. R. Soc. London Ser.*, **B 352**, pp. 661–668, 1997.
10. A. Kienle, L. Lilge, and M. S. Patterson, R. Hibst, R. Steiner and B. C. Wilson, "Spatially resolved absolute diffuse reflectance measurements for noninvasive determination of the optical scattering and absorption coefficients of biological tissue," *Appl. Opt.*, **vol. 35**, pp. 2304–2314, 1996.
11. J. R. Mourant, I. J. Bigio, D. A. Jack, T. M. Johnson, and H. D. Miller, "Measuring absorption coefficients in small volumes of highly scattering media: source-detector separations that do not depend on scattering properties," *Appl. Opt.*, **vol. 36**, pp. 5655–5661, 1997.
12. M. G. Nichols, E. L. Hull, and T. H. Foster, "Design and testing of a white-light, steady-state diffuse reflectance spectrometer for determination of optical properties in highly scattering systems," *Appl. Opt.*, **vol. 36**, pp. 93–104, 1997.
13. M. S. Patterson, B. Chance and B. C. Wilson, "Time resolved reflectance and transmittance for the non-invasive measurement of tissue optical properties," *Appl. Opt.*, **vol. 28**, pp. 2331–2336, 1989.
14. B. W. Pogue and M. S. Patterson, "Frequency-domain optical absorption spectroscopy of finite tissue volumes using diffusion theory," *Phys. Med. Biol.*, **vol. 39**, pp. 1157–1180, 1994.
15. R. Cubeddu, A. Pifferi, P. Torricelli and G. Valentini, "Experimental test of theoretical models for time-resolved reflectance," *Med. Phys.*, **vol. 23**, pp. 1625–1633, 1996
16. T. J. Farrell, M. S. Patterson, and B. Wilson, "A diffusion theory model of spatially resolved, steady-state reflectance for the noninvasive determination of tissue optical properties *in vivo*," *Med. Phys.*, **vol. 19**, pp. 879–888, 1992.
17. W. M. Star, "Diffusion theory of light transport," in *Optical-Thermal Response of Laser Irradiated Tissue*, A. J. Welch and M. J. C. van Gemert, Eds., chapter 6, pp. 131–205. Plenum Press, 1995.
18. S. L. Jacques and L. Wang, "Monte Carlo modeling of light transport in tissue," in *Optical-Thermal Response of Laser Irradiated Tissue*, A. J. Welch and M. J. C. van Gemert, Eds., chapter 4, pp. 73–99. Plenum Press, 1995.
19. T. J. Farrell, B. Wilson, and M. S. Patterson, "The use of neural network to determine tissue optical properties from spatially resolved diffuse reflectance measurements," *Phys. Med. Biol.*, **vol. 37**, pp. 2281–2286, 1992.
20. J. S. Dam, T. Dalgaard, P. E. Fabricius and S. Andersson-Engels, "Multiple polynomial regression method for determination of biomedical optical properties from integrating sphere measurements," *Appl. Opt.*, **vol. 39**, pp. 1202–1209, 2000.

21. G. H. Weiss, R. Nossal, and W. F. Bonner, "Statistics of penetration depth of photons re-emitted from irradiated tissue," *J. Modern Optics*, **vol. 36**, pp. 349–359, 1989.
22. M. S. Patterson, S. Anderson-Engels, B. C. Wilson, and E. K. Osei, "Absorption spectroscopy in tissue-simulating materials: a theoretical and experimental study of photon paths," *Appl. Opt.*, **vol. 34**, pp. 22–30, 1995.
23. F. Bevilacqua, D. Piquet, P. Marquet, J. D. Gross, B. J. Tromberg, and C. Despeursinge, "*In vivo* local determination of tissue optical properties: applications to the human brain," *Appl. Opt.*, **vol. 38**, pp. 4939–4950, 1999.
24. S. A. Prahl and S. L. Jacques, "Sized-fiber spectroscopy," in *SPIE Proceedings of Laser Tissue Interaction IX*, S. L. Jacques, Ed., vol. 3254, pp. 348–352, SPIE, Bellingham, 1998.
25. T. P. Moffitt and S. A. Prahl, "In vivo sized-fiber spectroscopy," in *SPIE Proceedings of Optical Biopsy III*, R. R. Alfano, Ed., vol. 3917, pp. 225–231, SPIE, Bellingham, 2000.
26. S. T. Flock, S. L. Jacques, B. C. Wilson, W. M. Star, and M. J. C. van Gemert, "Optical properties of intralipid: A phantom medium for light propagation studies," *Lasers Surg. Med.*, **vol. 12**, pp. 510–519, 1992.
27. J. W. Pickering, S. A. Prahl, N. van Wieringen, J. F. Beek, H. J. C. M. Sterenborg, and M. J. C. van Gemert, "Double-integrating-sphere system for measuring the optical properties of tissue," *Appl. Opt.*, **vol. 32**, pp. 399–410, 1993.
28. S. A. Prahl, M. J. C. van Gemert and A. J. Welch "Determining the optical properties of turbid media by using the adding-doubling method," *Appl. Opt.*, **vol. 32**, pp. 559–568, 1993.
29. H. J. van Staveren, C. J. M. Moes, J. van Marle, S. A. Prahl, and M. J. C. van Gemert, "Light scattering in Intralipid-10% in the wavelength range of 400–1100 nm," *Appl. Opt.*, **vol. 31**, pp. 4507–4514, 1991.
30. J. P. A. Marijnissen, W. M. Star, J. L. van Delft, and N. A. P. Franken, "Light intensity measurements in optical phantoms and *in vivo* during HpD photoradiation treatment using a miniature light detector with isotropic response," in *Photodynamic Therapy of Tumors and other Diseases*, G. Jori and C. Perria, Eds., pp. 387–390. Libreria Progetto, Padova, Italy, 1985.
31. W. F. Cheong, S. A. Prahl, and A. J. Welch, "A review of the optical properties of biological tissues," *IEEE J. Quantum Electron.*, **vol. 26**, pp. 2166–2185, 1990.
32. B. W. Pogue and G. Burke, "Fiber-optic bundle design for quantitative fluorescence measurement from tissue," *Appl. Opt.*, **vol. 37**, pp. 7429–7436, 1998.
33. R. R. Anderson and J. A. Parrish, "The optics of human skin," *J. Invest. Derm.*, **vol. 77**, pp. 13–19, 1981.
34. T. P. Moffitt and S. A. Prahl, "Sized-fiber reflectometry for measuring local optical properties," *IEEE J.S.T.Q.E.*, in press.